Rare Metal Materials and Engineering
Volume 52, Issue 6, June 2023
Available online at www.rmme.ac.cn

Science Press

Cite this article as: Gao Zhongtang, Yu Defeng, Gao Zhiming, et al. Effect of Melt Hydrogen Content on Hot Tearing Behavior of Al-Cu Alloys[J]. Rare Metal Materials and Engineering, 2023, 52(06): 2039-2047.

ARTICLE

Effect of Melt Hydrogen Content on Hot Tearing Behavior of Al-Cu Alloys

Gao Zhongtang[1], Yu Defeng[1], Gao Zhiming[1], Lu Jiawei[1], Yu Yuan[2], Zhang Chuanwei[1]

[1] School of Mechanical Engineering, Xi'an University of Science and Technology, Xi'an 710054, China; [2] State Key Laboratory of Solid Lubrication, Lanzhou Institute of Chemical Physics, Chinese Academy of Sciences, Lanzhou 730000, China

Abstract: Al-Cu alloy with wide solidification interval is prone to hot tearing and porosity defects due to insufficient feeding. The effect of hydrogen content on the hot tearing susceptibility (HTS) of Al-*x*Cu alloy was investigated by the constrained rod casting (CRC) mold. Based on analysis of the HTS value, fracture morphology and the microstructure of Al-*x*Cu alloy with different hydrogen contents in the melt, the influence of porosity formation on the hot tearing was analyzed. The results show that the hot tearing susceptibility of the alloy is evidently aggravated, which is caused by grain coarsening and insufficient feeding of liquid phase in the late stage of solidification with the increase in melt hydrogen content. A porosity-based formation mechanism of hot tearing is proposed to explain the interplay between porosity and hot tearing.

Key words: Al-Cu alloy; hydrogen; hot tearing susceptibility; casting; porosity

Owing to the excellent mechanical properties, high fatigue strength and distinguished corrosion resistance[1–3], aluminum-copper (Al-Cu) alloys have become an important light material in automobile field[4], and are also widely used in the fields of aerospace and shipbuilding[5–7]. However, Al-Cu alloys have poor casting characteristics, especially the long freezing range, poor fluidity and high hot tearing susceptibility (HTS), which greatly restrain their application in the industry[8–10]. Another disadvantage of Al-Cu alloys is the high uncertainty of their mechanical behavior due to casting-related defects such as porosity and entrained oxide bi-film[11–12].

As the major defects in the casting process, hot tearing and porosity are detrimental to the product quality. According to the previous researches, hot tearing is caused by the combined effect of insufficient feeding and interdendritic stress concentration in the mushy zone[13–16]. Campbell[17] pointed out that the porosity is caused by the combination of the reduction of hydrostatic pressure in the mushy and the segregation of dissolved gases (hydrogen[18], nitrogen and carbon monoxide). The depression is associated with the insufficient feeding[19–20]. Many studies [21–22] have shown that both defects are induced by the insufficient feeding at the end of solidification, and there is a certain correlation in the formation process.

Numerous researches have proposed that porosity plays a key role in the formation of hot tearing. M'Hamdi et al[23] found that the increase in porosity level in DC casting of aluminum alloys resultes from the thermally induced deformation, which increases the hot tearing susceptibility. Hence, they proposed that thermally induced "opening-up" of the pores might be an important reason for the hot tearing formation. Terzi et al[24] observed the deformation behavior of the Al-Cu alloys in the semi-solid state using ultrafast and high-resolution X-ray micro-tomography. It is shown that once the liquid is no longer capable to feed the intergranular surface perpendicular to the strain axis, pores will form and grow, which results in cracks. Phillion et al[25] investigated the semi-solid deformation of Al-12wt% Cu alloy by in-situ method of real-time synchrotron X-ray. It is found that the radiographic observations are consistent with classical hot tearing behavior at higher fraction solids. The void nucleates and gathers, and finally forms cracks. Coniglio and Cross[26] proposed that cracks may initiate from pores in the coherent region of dendrites. The formation of pores depends on

Received date: November 21, 2022
Foundation item: National Natural Science Foundation of China (51804251, 52104384); Science Fund of Shandong Laboratory of Yantai Advanced Materials and Green Manufacturing (AMGM2021F04); Planning Project of Xi'an Science and Technology (21XJZZ0041); China Postdoctoral Science Foundation (2020M683675XB); NSF of Shaanxi Provincial Department of Education (21JK0761); Key Research and Development Program of Shaanxi (2023-YBGY-343)
Corresponding author: Gao Zhiming, Ph. D., Associate Professor, School of Mechanical Engineering, Xi'an University of Science and Technology, Xi'an 710054, P. R. China, Tel: 0086-29-85583157, E-mail: gaozm@xust.edu.cn

whether the content of dissolved gas exceeds its solubility. In addition, they proposed the porosity-based crack initiation model and the hot tearing propagation model combined with the mass balance. It shows that gas concentration and strain rate determine the crack initiation and growth.

The previous research indicates that there is a close relation between the formation mechanisms of hot tearing and porosity. The nucleation and growth of porosity and hot cracks proceed simultaneously during the solidification of alloys. And porosity and hot tearing show competitive growth in the final stage of solidification. Few studies have clarified the potential correlation between porosity and hot tearing[27–28]. In this work, Al-Cu alloys were chosen to investigate the correlation between porosity and hot tearing. The effect of porosity on the hot tearing susceptibility was studied by the change of the hydrogen content in the melt. The microstructure evolution of Al-*x*Cu alloy was also analyzed to explicate the evolution of porosity and hot cracks. A porosity-based hot tearing initiation model was proposed to clarify the correlation between porosity and hot tearing.

1 Experiment

1.1 Alloy preparation

Al-*x*Cu (*x*=1, 2, 3.3, 4.3, wt%) alloys were prepared in an electrical furnace with 99.99% Al and Al-Cu master alloy with 51.87% Cu. The alloy was completely melted and the liquid metal was stirred. Then the molten alloy was exposed to the atmosphere and held at 730 °C for 5 min to reach a dynamic equilibrium of hydrogen content between the moist air and melt. Before pouring, the slag on the surface of molten metal was stripped out. Since the present work aims to investigate the effect of melt gas content on hot tearing susceptibility, there is no degassing process in this experiment.

1.2 Assessment of hot tearing performance

The hot tearing tests were carried out in the constrained rod casting (CRC) mold, which was similar to the one previously used by other researchers[29–32] for determining the hot tearing. Detailed specifications of the mold are shown in Fig.1. There are four rods with 9.5 mm in diameter distributed on the runner, with lengths of 51, 89, 127 and 165 mm. The end of each rod is a ball with 19 mm in diameter to limit the shrinkage of the melt after solidification. The flow channel of the CRC mold was coated with ZnO and preheated to 200 °C. The melt was poured at 710 °C and the cooling curve of the casting was monitored with K-type thermal couple and YOKOGAWA recorder.

1.3 Melt hydrogen content measurement

A rapid gas measuring device was used to determine the hydrogen content of aluminum alloy melt. Fig. 2a is the schematic diagram of measuring instrument. After the melt was poured into the small crucible, the bell jar was closed and the vacuum pump was turned on to get the melt solidified under the preset vacuum conditions. The vacuum degree should be set to a value to ensure no bubbles exiting from the surface of the ingot during solidification, and all hydrogen

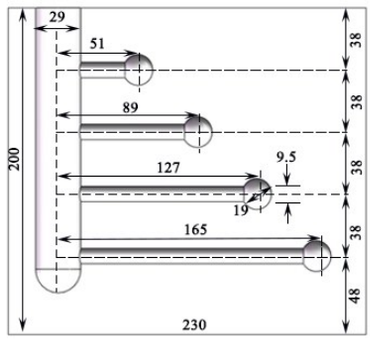

Fig.1 Mold for constrained rod casting (CRC)

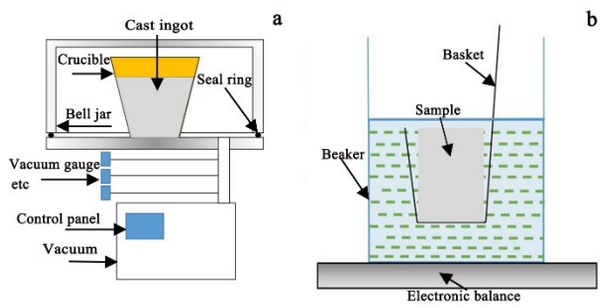

Fig.2 Schematic diagrams of hydrogen measuring device (a) and Archimedes' law (b)

will remain in the melt. Based on the above methods, the solidified samples under atmospheric pressure and preset vacuum conditions were obtained.

The density of the sample was obtained by Archimedes' law[33]. The mass of the sample was measured and the sample was immersed into the alcohol with the self-made basket to measure apparent mass of the sample. The schematic diagram is shown in Fig.2b. The density of sample can be obtained by Eq.(1).

$$\rho = m\rho_1/(m - m_1) \quad (1)$$

where ρ is the density of the aluminum alloy; ρ_1 is the density of alcohol (~0.789 g/cm^3); m and m_1 is the mass of the sample and the apparent mass of the sample immersed in alcohol (measured by an electronic balance with an accuracy of ±0.0001 g), respectively.

Then the hydrogen content in the melt is calculated by Eq.(2)[34].

$$C_H = 100\frac{P_2}{P_1}\left(\frac{1}{\rho} - \frac{1}{\rho_0}\right) \quad (2)$$

where C_H is the density index, mL/100g; ρ_0 is the density of the sample solidified under an atmospheric pressure and ρ is the density of the sample solidified under a preset vacuum condition; P_1 is a standard atmospheric pressure, MPa; P_2 is a reduced pressure, MPa.

1.4 Sample preparation

The sample was cut from a representative bar of each group in experiment, as shown in Fig.3. Sample 1# was cut from the right arm of the bar. The incomplete breaking bar was

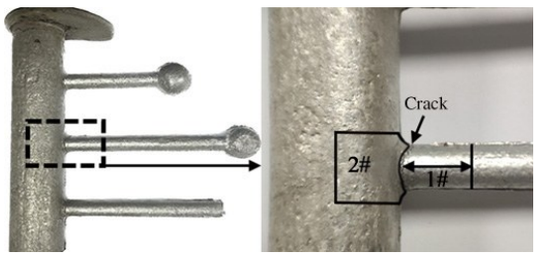

Fig.3 Sampling position for the OM and SEM observation

intentionally snapped to acquire the torn fracture surface. The scanning electron microscopy (SEM) was used to observe the axial cross-section morphology of the fracture surface. Sample 2# was cut from the sprue conjunction region along the center line of the bar to observe the pores and cracks near the fracture. The longitudinal cross section was ground with grinding papers and polished before etching with Keller's agent. The samples were examined by optical microscopy (OM) to analyze the microstructure, amount, morphology and distribution of pores.

2 Results and Discussion

2.1 Hot tearing susceptibility

The visible cracks of Al-*x*Cu alloys with different melt hydrogen contents are shown in Fig.4. The degree of cracks is firstly severe and then weakened with the increase in copper content. However, the fracture of Al-*x*Cu alloys with high melt gas content is more serious than that of the alloys with low hydrogen content. The hot tearing tendency of Al-*x*Cu alloys increases first and then decreases with the increase in copper content and is not affected by the change of melt gas content. The hot tearing tendency is judged by the number of fractures and the severity of crack. However, it is difficult to judge the hot tearing susceptibility only from the fracture. Hot tearing sensitivity of samples with different copper concentrations and hydrogen contents was quantitatively compared by Argo calculation formula.

The constrained bar method is used to evaluate the hot tearing susceptibility (HTS) of Al-Cu alloys. The HTS value is evaluated by Argo[35–36] calculation formula:

$$\mathrm{HTS} = \sum\left(f_{\mathrm{length}} \times f_{\mathrm{crack}} \times f_{\mathrm{location}}\right) \quad (3)$$

where HTS is the overall hot tearing sensitivity of alloy casting; f_{length} is the bar length at which the crack occurs, and the values of 4, 8, 16 and 32 for f_{length} represent the longest hot tearing rod, the second-longest rod, the second shortest rod and the shortest rod, respectively; f_{crack} is hot crack severity, and the values of 1, 2, 3 and 4 for f_{crack} represent the hairline crack, the slight crack, the severe crack and the complete separation, respectively; f_{location} is the hot crack location, the values of 1, 2 and 3 for f_{location} represent crack at the rod end, the ball end, and the middle of the rod, respectively. The acquisitions of f_{length}, f_{crack} and f_{location} are shown in Fig.5.

The HTS values of Al-*x*Cu alloys with different hydrogen contents are shown in Fig. 6. The alteration of hydrogen content in melt is achieved by changing the humidity of the atmosphere. The measured hydrogen values are categorized into two levels, the low hydrogen content and the high hydrogen content, as shown in Table 1. It is obvious in Fig. 6 that the HTS value of alloys with high hydrogen content is significantly higher than that of alloys with low hydrogen content, and the hot tearing susceptibility first increases and then decreases with the increase in copper concentration. Al-2Cu alloy has the highest hot tearing sensitivity regardless of hydrogen content. The results of HTS value are consistent with those observed in the macro morphology. To further study the influence of hydrogen content in the melt on hot tearing sensitivity, the micro morphology of cross section of samples is observed.

2.2 Fracture morphology

The SEM images of the center areas of fracture surface taken at a lower magnification are shown in Fig. 7. The solidification model is columnar as seen in Fig. 7a. It can be

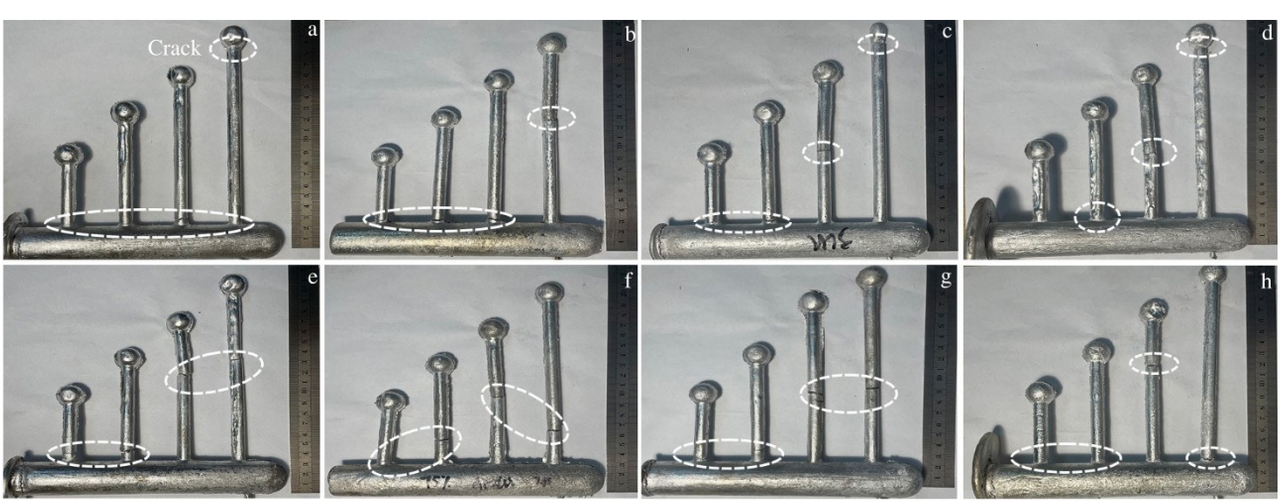

Fig.4 CRC test samples of Al-*x*Cu alloys with low hydrogen content (a–d) and high hydrogen content (e–h) : (a, e) *x*=1, (b, f) *x*=2, (c, g) *x*=3.3, and (d, h) *x*=4.3

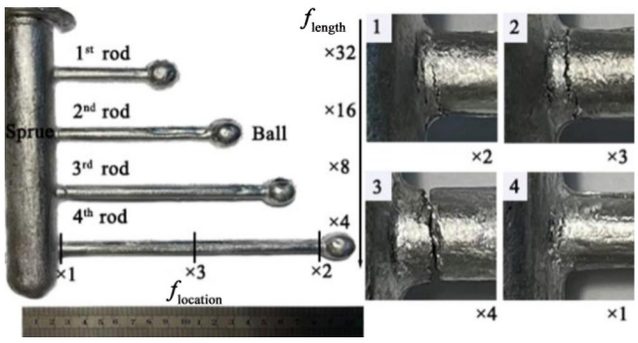

Fig.5 Determine of HTS from crack characteristics in terms of f_{length}, f_{crack} and $f_{location}$

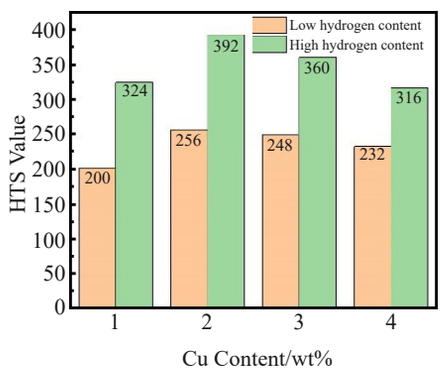

Fig.6 HTS of Al-*x*Cu alloys with different hydrogen contents in melt

seen that there is liquid film among the dendrites on the fracture surface from the enlarged view of Fig. 7b. The liquid film on the grain surface is formed by the final solidification of the low melting point phase. According to the liquid film theory[37], the formation of hot tearing is caused by the liquid film cracking due to the destruction of the bonding force of the liquid film between grains because of the solidification shrinkage stress at the end of solidification. According to HTS value in Fig. 6, the sensitivity of hot tearing increases with the increase in liquid film when the content of Cu is less than 2wt%, which agrees with the liquid film theory. The solidification model of Al-1Cu alloy with high hydrogen content is columnar and there is pore on fracture surface, as shown in Fig. 7c. The axial cracks are visible in holes and connected by many small pores. The increase in the dissolved hydrogen content in the melt causes plenty intergranular bubbles to form pores[38]. It can be seen from Fig. 6 that the hot tearing sensitivity of the Al-1Cu alloys increases with the increase in the melt gas content. Pores are related to the formation of hot tearing and have a positive effect on hot tearing sensitivity. Besides, there are some protuberances on the grain surface as shown in Fig. 7d. The related studies[39–40] reveal that it is a fully broken intergranular bridge. It indicates that the bonding force of the alloy is not enough to resist the shrinkage stress, and finally the hot tearing defect is formed. However, the bonding force decreases with the increase in interdendritic

Table 1 Hydrogen content of samples at different humidity (mL/100g)

Cu content	1wt%	2wt%	3.3wt%	4.3wt%
Low hydrogen	0.5764	0.6299	0.8321	0.6102
High hydrogen	0.9116	0.9429	2.0001	1.0396

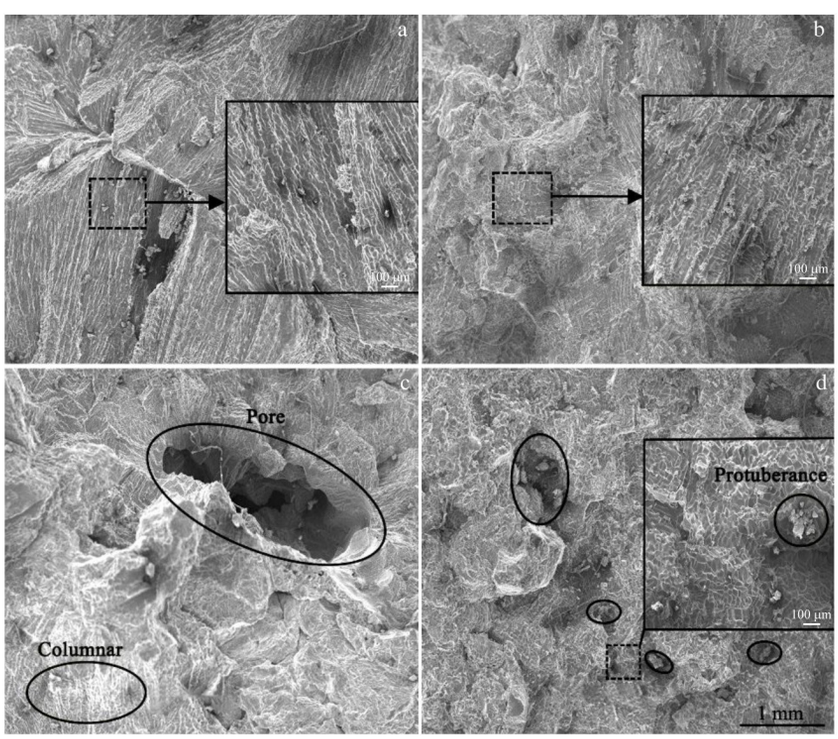

Fig.7 SEM micrographs of fracture of Al-*x*Cu with low hydrogen content (a, b) and high hydrogen content (c, d): (a, c) *x*=1 and (b, d) *x*=2

pores which are caused by the increase in melt gas content. Therefore, the increase in interdendritic pores increases the hot tearing sensitivity. The HTS value of Al-2Cu alloys also reaches the highest in Fig. 6. The fracture surface is rough at low copper concentration and there are no regions of eutectics covering the surface as shown in Fig. 7. It can be seen that the fracture surface becomes coarse and there are more ruptured solid bridges with the increase in hydrogen content in the melt.

To further reveal the microstructure of facture and interdendritic porosities, SEM images of fracture surface from the center areas taken at a higher magnification are shown in Fig. 8. There are porosities on the hot tear surface, which prevents the continuous flow of liquid in the final stage of solidification. The researchers[41–42] confirm that the roughness of the fracture surface is composed of additional dendrite arm tips. The hot tearing is formed by breaking the contact between dendrites when the temperature is lower than the melting point temperature. However, the liquid film is sufficient to promote the formation of the dendritic tip during interdendritic separation. And liquid folds on the fracture surface can be observed in Fig. 8a. The connected solid bridge and partially discrete spikes on the tearing surface are shown in Fig. 8b. These spikes are signs of solid bridging in dendrites that are elongated before fracture occurs. These spikes can be deformed during solidification of the last remaining interdendritic liquid[43]. There are obvious eutectic phase and spikes in the fracture morphology of Al-3.3Cu alloy, as shown in Fig. 8c. There are more eutectic phases with low melting point and the thicker liquid films are formed in dendrite boundaries with the increase in Cu content, which enhance the feeding ability for dendrite separation and improve the bonding ability between dendrites. Therefore, the hot tearing tendency of the alloy decreases, consistent with the result of Fig. 6. The detached solid bridges and the larger porosity among the bumpy surface are shown in Fig. 8d. The porosity causes the lack of liquid in interdendritic area, so almost all solidified particles in mushy area are separated by liquid film. The typical eutectic meniscus and obvious ruptured liquid film are shown in Fig. 8e. The Al-3.3Cu alloy fracture surface also has the eutectic phases (Fig. 8f). The thickness and fold degree of liquid film decrease with the increase in hydrogen content from the fracture morphology. Therefore, the alloy can withstand lower solidification shrinkage stress to increase the hot tearing susceptibility. In addition, the porosity size of high hydrogen content samples is larger than that of low hydrogen content sample, which hinders the flow feeding of the liquid phase alloy and decreases the bonding force of alloy.

The porosity-related hot tearing mechanism proposed by the previous researchers[26–28] indicates that the formation of porosity plays an important role in the evolution of hot tearing. The observation of the fracture surface of Al-*x*Cu alloy casting by SEM is shown in Fig. 8. It is found that hot tear is formed by coalescence of the porosity. Hence, the formation mechanism of hot tearing is proposed and demonstrated in Fig. 9. Firstly, pores nucleate on folded, entrained oxide biofilms or dendrite arms, which are frequently considered as the nucleation of hot tearing (Fig. 9a). Then, the pores grow in interdendritic grooves (Fig. 9b). Because they are not completely constrained by the solid network at the early stage of growth, their shape is spherical. The gas continuously overflows from the growing dendrite arms and diffuses into pores. The pores grow continuously

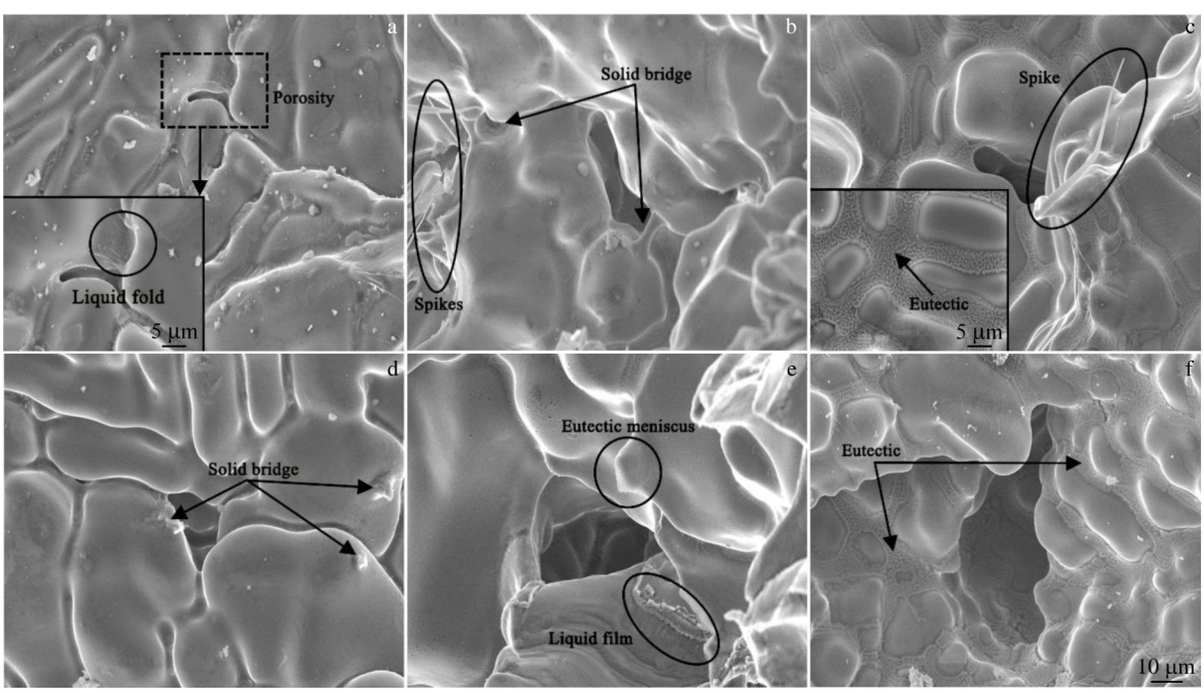

Fig.8 SEM micrographs at higher magnification of the fracture of Al-*x*Cu with low hydrogen content (a–c) and high hydrogen content (d–f): (a, d) *x*=1, (b, e) *x*=2, and (c, f) *x*=3.3

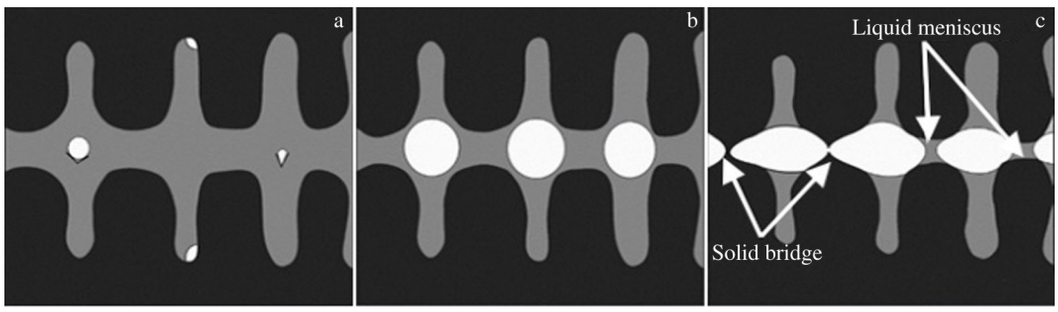

Fig.9 Porosity-based mechanism for hot tearing formation: (a) nucleation, (b) growth and (c) coalescence

and impinge the surrounding dendrite arms that are gradually narrowing. Finally, pores tend to coalesce with the nearby ones and form a short-range crack along the grain boundary (Fig. 9c). Consequently, the coalescence of porosity can be seen as the propagation mechanism for hot tearing. An elevated fraction of porosity tends to promote the formation of hot tearing by reducing the solid bridges and decreasing the feeding flow. Therefore, the porosity-based hot tearing mechanism means that porosity is crucial to the formation of hot tearing.

2.3 Microstructure of cross section

In order to confirm the porosity-based hot tearing mechanism, the longitudinal cross section near the fracture surface is characterized. The optical macrographs and micrographs of cross section specimen are shown in Fig. 10. The optical micrograph of location A in Fig.10a_1 is enlarged in Fig. 10a_2. The crack is propagated along the boundary of coarse grains. The optical micrograph of location A with larger magnification is shown in Fig. 10a_3. Several small cracks are observed in the interdendritic interface. The size of grain becomes smaller when the copper content increases to

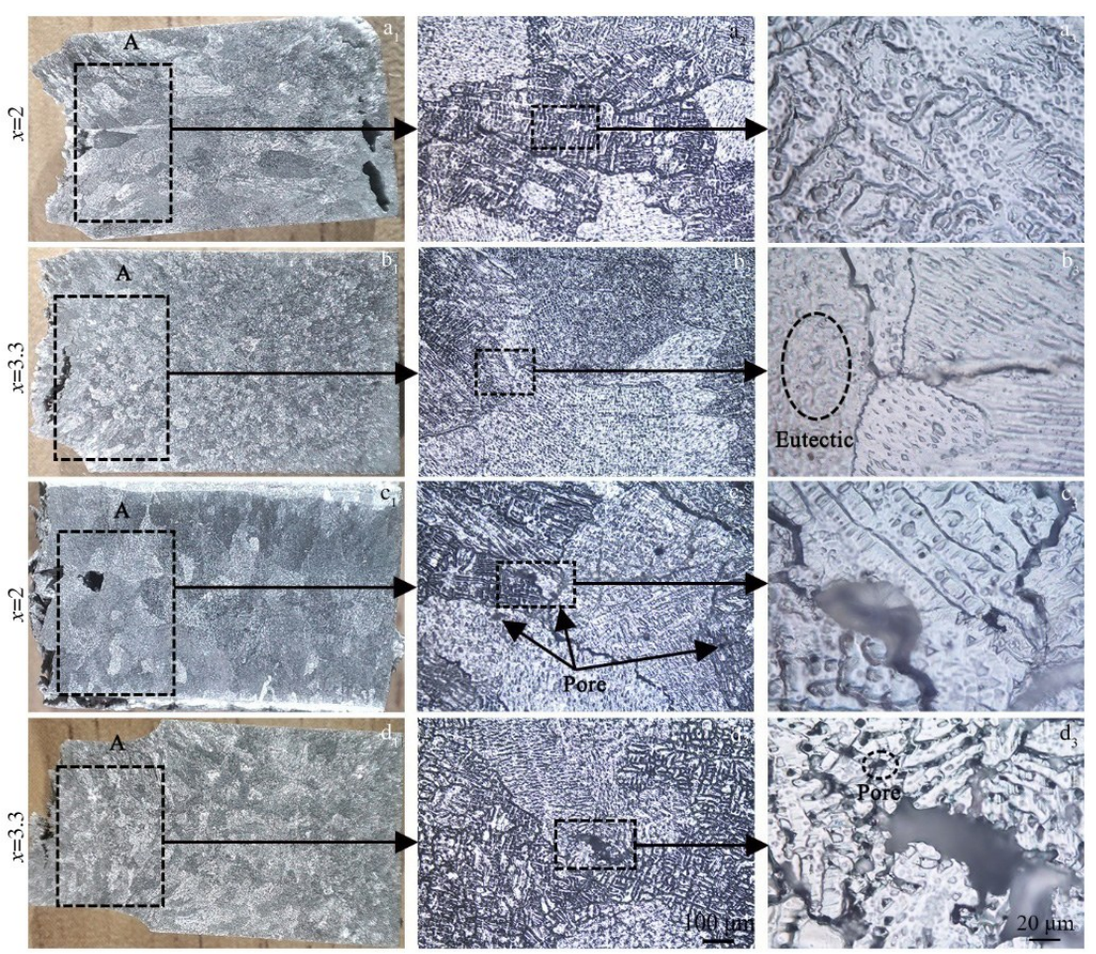

Fig.10 Optical macrographs of fracture cross-section of Al-*x*Cu alloy with low hydrogen content (a_1–a_3, b_1–b_3) and high hydrogen content (c_1–c_3, d_1–d_3)

3.3wt% , as shown in Fig. 10b_1. In order to get a clearer analysis of microstructure evolution, Fig. 10b_1 is magnified as shown in Fig. 10b_2. The microstructure in Fig. 10b_2 is obviously fined compared with Fig. 10a_2. Meanwhile, the eutectic phase can be found in the microstructure, as shown in Fig. 10b_3. To analyze the effect of hydrogen content on microstructure evolution, the microstructure of the Al-2Cu with high hydrogen content in Fig. 10c_1 has coarser grains compared with that of the low hydrogen content sample in Fig. 10a_1. Meanwhile, there are some pores in Fig. 10c_2 and the pores coalesce to form larger cracks (Fig. 10c_3), which increases the HTS. The grain size of Al-3.3Cu with high hydrogen content decreases as shown in Fig. 10d_1 and 10d_2. It can be seen in Fig. 10d_3 that there are large pores and cracks at the grain boundary and many small pores exist between dendrites arms.

The above results of microstructure analysis confirm the validity and effectiveness of the porosity-based hot tearing model. The pores overflow from interdendritic arms and finally coalesce to form cracks along the boundary. The Al-2Cu alloy has the most cracks and the coarsest grain as shown in Fig. 10. The coarse grains cause severe stress concentration, which leads to the high HTS. Compared with aluminum-copper alloy with different hydrogen contents, high hydrogen content greatly increases the number of pores and coarsens the grains to a certain extent. The reaction between aluminum and water vapor is intensified with the increase in humidity, which results in the increase in hydrogen and oxide in the melt. The heterogeneous nucleation is promoted with the increase in oxide coarse grains.

The Al-2Cu alloy with high hydrogen content is further analyzed in Fig. 11. The axial cross-section of sample is divided into three parts: location A (close to the fracture, Fig. 11a_1 and 11a_2), location B (in the middle, Fig. 11b_1 and 11b_2), location C (far from the fracture, Fig. 11c_1 and 11c_2).

Distinct cracks appear in location A along the grain boundary, as shown in Fig. 11a_1. The cracks become smaller or even disappear in the location B (Fig. 11b_1). There are some coarse dendrites and no cracks in location C (Fig. 11c_1) due to the final solidification position near the sprue. Fig. 11a_2, 11b_2 and 11c_2 are optical macrographs at high magnification of location A, B and C, respectively. It can be found that both the number and the size of pores increase with the distance from the fracture surface. This is due to the fact that most of pores at location A are coalesced together to form hot cracks. And only small part of pores at location B are consumed. Whereas the pores in position C are almost all retained. The pores coalesce to form hot cracks. Then hot cracks elongate by consuming the pores in the adjacent areas[44–46]. Therefore, pores play a key role in the nucleation and growth process of hot cracks.

The results show that there are many cracks near the fracture surface at location A, and some cracks are connected with pores. It can be seen that hot cracks usually extend along

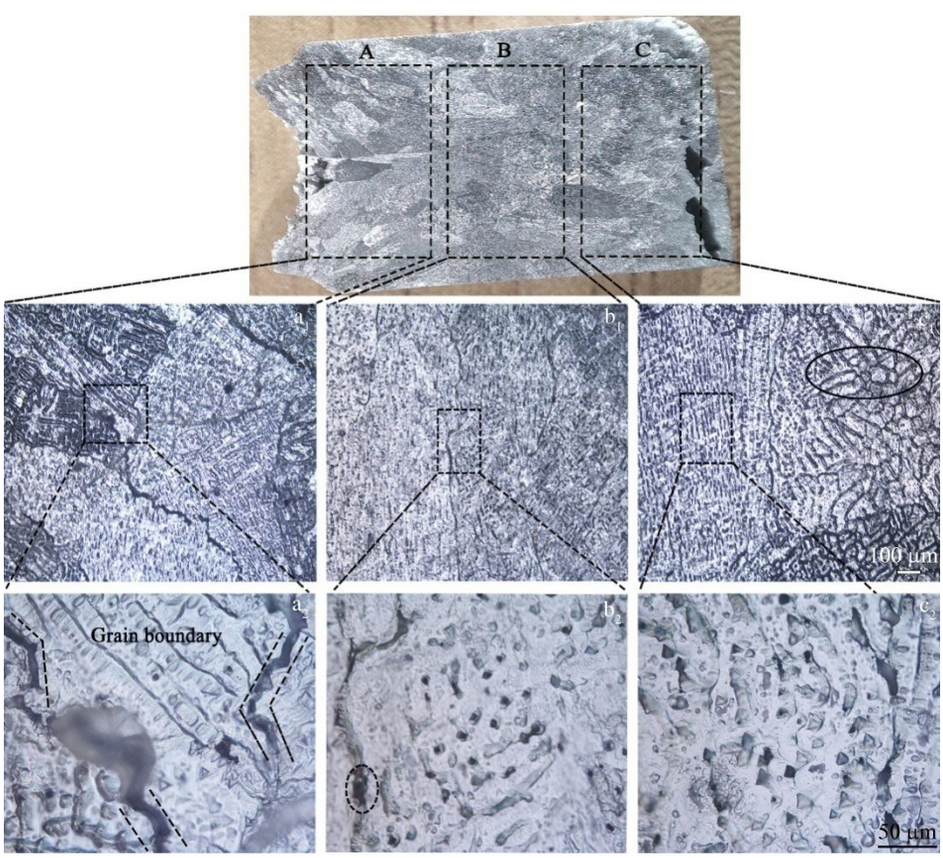

Fig.11 Optical macrographs of Al-2Cu with hydrogen content of 0.9429 mL/100g: (a_1, a_2) location A, (b_1, b_2) location B, and (c_1, c_2) location C

the grain boundary and some cracks are connected by holes. Therefore, it can be seen that many unconsumed pores are distributed in interdendrites and there are more cracks in the sample with higher hydrogen content. The nucleation of pores can be regarded as the nucleation of hot cracks.

3 Conclusions

1) The hot tearing susceptibility (HTS) of Al-Cu alloy is firstly strengthened and then weakened with the increase in copper content. The HTS value of the alloys with high hydrogen content obviously increases, indicating that the thermal cracking sensitivity is positively correlated with hydrogen content.

2) The increase in hydrogen content in melt changes the size and number of pores. The porosity leads to the insufficient feeding of interdendritic liquid. Therefore, the hot tearing susceptibility of Al-Cu alloy increases.

3) The experimental results of microstructure analysis demonstrate the validity and correctness of the porosity-based hot tearing model. The nucleation process of pores can be considered as the nucleation process of hot tearing. Pores close to the fracture surface coalesce to form a short-range hot crack.

References

1 Akhyar H, Malau V, Suyitno *et al. Results in Physics*[J], 2017, 7: 1030

2 Lotfy A, Pozdinakov A V, Zolotorevskiy V S *et al. Materials Characterization*[J], 2018, 136: 144

3 D ' Elia F, Ravindran C, Sediako D. *Materials Science and Engineering A*[J], 2015, 624: 169

4 Sujith S V, Mahapatra M M, Mulik R S. *Transactions of the Indian Institute of Metals*[J], 2018, 71(4): 923

5 Li M, Wang H W, Wei Z J *et al. Materials & Design*[J], 2010, 31(5): 2483

6 Wang Y X, Yue C Y, Su M *et al. Journal of Materials Engineering and Performance*[J], 2022, 31: 6349

7 Gao Z T, Ren H B, Geng H M *et al. Journal of Materials Engineering and Performance*[J], 2022, 31: 9534

8 Huang S Y, Wang C X, He K Z *et al. Philosophical Magazine Letters*[J], 2019, 99(12): 444

9 Liu J W, Kou S D. *Acta Materialia*[J], 2016, 110: 84

10 Uludag M, Cetin R, Dispinar D. *Metallurgical and Materials Transactions A*[J], 2018, 49(5): 1948

11 Bagherpoor-Torghabe H, Niroumand B, Karbasi M. *The International Journal of Advanced Manufacturing Technology*[J], 2014, 75(5–8): 677

12 Dou R F, Phillion A B. *Metallurgical and Materials Transactions A*[J], 2016, 47(8): 4217

13 Katgerman L A. *Mathematical Model for Hot Cracking of Aluminium Alloys During DC Casting*[M]. New York: John Wiley & Sons, Inc, 2013

14 Suyitno, Pujiyulianto E, Arifvianto B *et al. Materials Science and Technology*[J], 2022, 38(5): 269

15 Li Y, Li H X, Katgerman L *et al. Progress in Materials Science*[J], 2021,117: 100 741

16 Wang M G, Pu Y. *Rare Metal Materials and Engineering*[J], 2017, 46(4): 946

17 Campbell J. *Materials Science and Technology*[J], 2013, 22(2): 127

18 Talbot D. *International Metallurgical Reviews*[J], 1975, 20(1): 166

19 Gao Z M, Jie W Q, Liu Y Q *et al. Acta Materialia*[J], 2017, 127: 277

20 Gao Z M, Jie W Q, Liu Y Q *et al. Journal of Alloys and Compounds*[J], 2019, 797: 514

21 Rappaz M, Drezet J M, Gremaud M. *Metallurgical and Materials Transactions A*[J], 1999, 30(2): 449

22 Sergio D, Felicelli *et al. Metallurgical & Materials Transactions B*[J], 2009, 40: 169

23 M ' Hamdi M, Mo A. *Materials Science and Engineering A*[J], 2005, 413–414: 105

24 Terzi S, Salvo L, Suery M *et al. Scripta Materialia*[J], 2009, 61(5): 449

25 Phillion A B, Hamilton R W, Fuloria D *et al. Acta Materialia*[J], 2011, 59(4): 1436

26 Coniglio N, Cross C E. *Materials Testing*[J], 2014, 56(7–8): 583

27 Suyitno, Kool W H, Katgerman L. *Micro-mechanical Model of Hot Tearing at Triple Junctions in DC Casting*[C]. Zurich-Uetikon: Trans Tech Publications Ltd, 2002

28 Coniglio N, Cross C E. *Metallurgical and Materials Transactions A*[J], 2009, 40(11): 2718

29 Hu B, Li D J, Li Z X *et al. Metallurgical and Materials Transactions A*[J], 2021, 52(2): 789

30 Shah A W, Ha S H, Kim B H *et al. Metallurgical and Materials Transactions A*[J], 2021, 52(8): 3353

31 Xu Y, Zhang Z, Gao Z *et al. Materials*[J], 2021, 14(22): 6881

32 Zou G, Chai Y, Shen Q *et al. International Journal of Metalcasting*[J], 2021, 16(2): 909

33 Mulazimoglu, Handiak N, Gruzleski Je. *AFS Trans*[J], 2008, 97: 225

34 Ni H J, Huang M Y, Zhu Y *et al. China Foundry*[J], 2004(S1): 7

35 Lin S, Aliravci C, Pekguleryuz M O. *Metallurgical and Materials Transactions A*[J], 2007, 38(5): 1056

36 Cao G, Kou S. *Materials Science and Engineering A*[J], 2006, 417(1–2): 230

37 Eskin D G, Katgerman L. *Metallurgical and Materials Transactions A*[J], 2007, 38(7): 1511

38 Opie W R, Grant N J. *JOM*[J],1950, 2(10): 1237

39 Zhou Y, Mao P L, Zhou L *et al. Journal of Magnesium and Alloys*[J], 2020, 8(4): 1176

40 Wang Z, Zhou Y, Li Y Z *et al. Transactions of Nonferrous Metals Society of China*[J], 2018, 28(8): 1504

41 Wang Z, Song J F, Huang Y D *et al. Metallurgical and Materials*

Transactions A[J], 2015, 46(5): 2108

42 Xu R F, Zheng H L, Luo J *et al. Transactions of Nonferrous Metals Society of China*[J], 2014, 24(7): 2203

43 Razaz G, Carlberg T. *Metallurgical and Materials Transactions A*[J], 2019, 50(8): 3842

44 Liang J, Jin Q L, Yang T W *et al. Rare Metal Materials and Engineering*[J], 2016, 45(10): 2519

45 Gao Z, Geng H, Qiao Z *et al*. *Ceramics International*[J], 2023, 49(4): 6409

46 Li S J, Zhan L H, Chen R *et al. Rare Metal Materials and Engineering*[J], 2016, 45(9): 2282

熔体氢含量对Al-Cu合金热裂行为的影响

高中堂[1]，余德锋[1]，高志明[1]，卢佳炜[1]，于　源[2]，张传伟[1]

(1. 西安科技大学 机械工程学院，陕西 西安 710054)

(2. 中国科学院兰州化学物理研究所 固体润滑国家重点实验室，甘肃 兰州 730000)

摘　要：Al-Cu合金具有较宽的凝固间隔，并且由于供给不足容易出现热裂和气孔缺陷。采用约束棒铸造（CRC）模具研究了氢含量对Al-*x*Cu合金热裂敏感性（HTS）的影响。通过分析熔体中不同氢含量的Al-*x*Cu合金的热裂敏感性值、断裂形态和微观结构，研究了孔隙形成对热裂行为的影响。结果表明，随着熔体氢含量的增加，合金在凝固后期由于晶粒粗化和液相供给不足，热裂敏感性明显增加。提出了一种基于孔隙率的热裂形成机制，以解释孔隙率和热裂之间的相互作用。

关键词：Al-Cu合金；含氢量；热裂敏感性；铸造；孔隙

作者简介：高中堂，男，1983年生，博士，副教授，西安科技大学机械工程学院，陕西 西安 710054，电话：029-85583159，E-mail：zhongtanggao@xust.edu.cn